REPORT

Cysteinyl-tRNA Synthetase Mutations Cause a Multi-System, Recessive Disease That Includes Microcephaly, Developmental Delay, and Brittle Hair and Nails

Molly E. Kuo,[1,2,11] Arjan F. Theil,[3,11] Anneke Kievit,[4] May Christine Malicdan,[5] Wendy J. Introne,[5] Thomas Christian,[6] Frans W. Verheijen,[4] Desiree E.C. Smith,[7] Marisa I. Mendes,[7] Lidia Hussaarts-Odijk,[4] Eric van der Meijden,[4] Marjon van Slegtenhorst,[4] Martina Wilke,[4] Wim Vermeulen,[3] Anja Raams,[3] Catherine Groden,[5] Shino Shimada,[5] Rebecca Meyer-Schuman,[8] Ya Ming Hou,[6] William A. Gahl,[5] Anthony Antonellis,[1,8,9,11,*] Gajja S. Salomons,[7,10,11,*] and Grazia M.S. Mancini[4,11]

Aminoacyl-tRNA synthetases (ARSs) are essential enzymes responsible for charging tRNA molecules with cognate amino acids. Consistent with the essential function and ubiquitous expression of ARSs, mutations in 32 of the 37 ARS-encoding loci cause severe, early-onset recessive phenotypes. Previous genetic and functional data suggest a loss-of-function mechanism; however, our understanding of the allelic and locus heterogeneity of ARS-related disease is incomplete. Cysteinyl-tRNA synthetase (*CARS*) encodes the enzyme that charges $tRNA^{Cys}$ with cysteine in the cytoplasm. To date, *CARS* variants have not been implicated in any human disease phenotype. Here, we report on four subjects from three families with complex syndromes that include microcephaly, developmental delay, and brittle hair and nails. Each affected person carries bi-allelic *CARS* variants: one individual is compound heterozygous for c.1138C>T (p.Gln380*) and c.1022G>A (p.Arg341His), two related individuals are compound heterozygous for c.1076C>T (p.Ser359Leu) and c.1199T>A (p.Leu400Gln), and one individual is homozygous for c.2061dup (p.Ser688Glnfs*2). Measurement of protein abundance, yeast complementation assays, and assessments of tRNA charging indicate that each *CARS* variant causes a loss-of-function effect. Compared to subjects with previously reported ARS-related diseases, individuals with bi-allelic *CARS* variants are unique in presenting with a brittle-hair-and-nail phenotype, which most likely reflects the high cysteine content in human keratins. In sum, our efforts implicate *CARS* variants in human inherited disease, expand the locus and clinical heterogeneity of ARS-related clinical phenotypes, and further support impaired tRNA charging as the primary mechanism of recessive ARS-related disease.

Aminoacyl-tRNA synthetases (ARSs) are essential, ubiquitously expressed enzymes that charge tRNA molecules with cognate amino acids in the cytoplasm and mitochondria.[1] Mutations in 32 ARS loci have been implicated in recessive disease, and the associated phenotypes tend to involve a wide array of tissues.[2–4] The genotypes of subjects with ARS-mediated recessive disorders suggest a loss-of-function mechanism for disease pathogenesis but are also consistent with the presumbed lethality of complete loss of ARS function. Specifically, subjects are compound heterozygous for one missense mutation and one null allele, compound heterozygous for two missense mutations, or homozygous for a single missense mutation.[2] Consistent with this notion, functional studies have revealed that recessive disease-associated ARS mutations cause reduced protein abundance in immunoblot assays,[5–17] decreased mutant enzyme activity via *in vitro* kinetic assays,[9,18–25] and/or diminished ability of the mutated gene to support cellular growth in yeast complementation assays.[12,13,21,22,26–33] As such, impaired protein translation as a consequence of decreased tRNA charging is the most likely molecular mechanism for ARS-mediated recessive disease.[2]

Here, we report on four affected individuals from three unrelated families. These individuals have similar clinical presentations (Table S1) and bi-allelic loss-of-function variants in cysteinyl-tRNA synthetase (*CARS* [MIM: 123859]). The appropriate, institute-specific review boards approved all studies, and informed consent was obtained from all subjects. The individual from family 1 (subject 1-3, Figure 1A) is of mixed European and French-Canadian descent and was enrolled in the NIH Undiagnosed Diseases Program. He was born at 33 weeks gestation to asymptomatic parents and presented with intrauterine growth retardation and microcephaly. In childhood he presented with failure to thrive, non-progressive cognitive delay, peripheral neuropathy, osteoporosis, proportionate short stature,

[1]Cellular and Molecular Biology Program, University of Michigan Medical School, Ann Arbor, MI 48109, USA; [2]Medical Scientist Training Program, University of Michigan Medical School, Ann Arbor, MI 48109, USA; [3]Department of Molecular Genetics, Oncode Institute, Erasmus Medical Center, University Medical Center Rotterdam, Dr. Molewaterplein 40, 3015 CN Rotterdam, the Netherlands; [4]Department of Clinical Genetics, Erasmus Medical Center, University Medical Center, 3015 GD Rotterdam, the Netherlands; [5]Undiagnosed Diseases Program and Office of the Clinical Director, National Human Genome Research Institute, National Institutes of Health, Bethesda, MD 20892, USA; [6]Department of Biochemistry and Molecular Biochemistry, Thomas Jefferson University, Philadelphia, PA 19107, USA; [7]Metabolic Unit, Department of Clinical Chemistry, Amsterdam University Medical Center and Amsterdam Gastroenterology and Metabolism, Vrije Universiteit Amsterdam, Amsterdam Neuroscience, 1081 HZ Amsterdam, the Netherlands; [8]Department of Human Genetics, University of Michigan Medical School, Ann Arbor, MI 48109, USA; [9]Department of Neurology, University of Michigan Medical School, Ann Arbor, MI 48109, USA; [10]Genetic Metabolic Diseases, Amsterdam University Medical Center, University of Amsterdam, 1081 HZ Amsterdam, the Netherlands
[11]These authors contributed equally
*Correspondence: antonell@umich.edu (A.A.), g.salomons@vumc.nl (G.S.S.)
https://doi.org/10.1016/j.ajhg.2019.01.006.

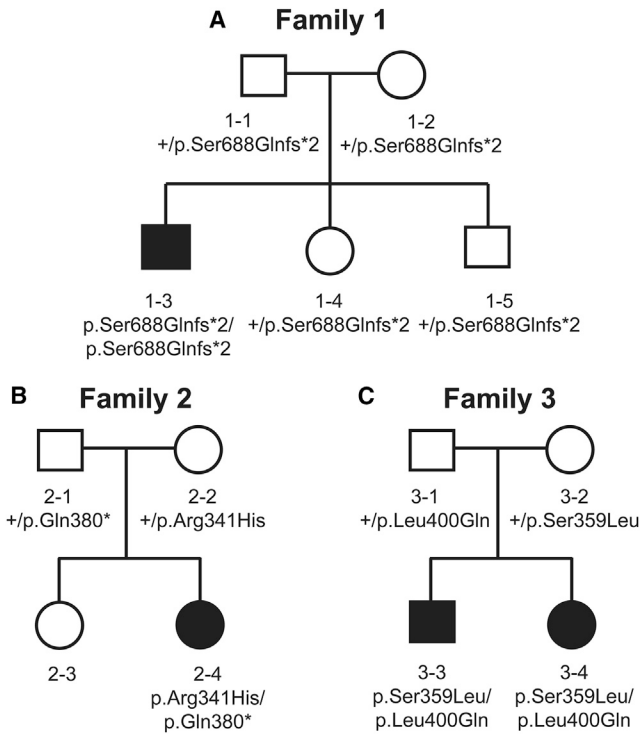

Figure 1. Pedigrees Harboring *CARS* Variants
Simplex pedigrees are shown for family 1 (A), family 2 (B), and family 3 (C). Squares represent males, and circles represent females. Subject numbers and genotypes are indicated under each symbol, and filled shapes indicate affected subjects.

recurrent hernias, mild aortic root dilatation, recurrent elbow dislocation, feeding difficulties, esophagitis requiring Nissen fundoplication, urinary retention, and chronic pain. At age 24 he was diagnosed with hypothalamic hypogonadism and delayed puberty, as well as type II diabetes mellitus. On examination he had dysmorphic features; a barrel-shaped trunk with wasting of the distal extremities; hypospadias with chordee; hyperextensible joints; myopia; central hypotonia but increased extremity tone; prominent lateral ventricles and sulci with mild cerebral atrophy upon brain MRI (Figures 2A–C); and fine, brittle hair (Figure 3A) and brittle nails (Figure S1A and S1B). Polarized light microscopy of hair shafts revealed moderate tiger-tail patterns compared to those of controls (Figures 4A and 4B). Subject 1-3 is currently 34 years old and has mild motor, language, and cognitive disabilities.

The individual from family 2 (subject 2-4, Figure 1B) is of Dutch descent, has asymptomatic parents, and was born at 38 weeks' gestation via elective cesarean section prompted by intrauterine growth retardation. As a result of a small atrial septal defect and failure to thrive, she was hospitalized for two months after birth. In childhood she developed restless behavior, poor sleep, mild dystonia, ataxic hand movements, poor coordination, and developmental delay. At age 30 she was diagnosed with diabetes mellitus. A CT scan of the head when she was 2 years old was normal. A brain MRI performed when she was 20 years old revealed areas of apparent delayed myelination; decreased white-matter volume; prominence of cerebellar folia; a small corpus striatum; hypoplasia of the corpus callosum; and mild, globally diffuse cerebral and cerebellar atrophy (Figures 2D–2F). The quality of the MRI and the lack of a repeat MRI did not allow distinction between hypomyelination and demyelination. On examination she had microcephaly; fine facial features; fragile nails; and sparse, brittle, and thin hair (Figure 3B). Light microscopy of hair shafts revealed trichoschisis and trichorrhexis nodosa, polarized microscopy showed weak but consistent tiger tail banding (Figure 4C), and scanning electron microscopy showed longitudinal grooves (data not shown). Subject 2-4 is currently 35 years old and has a moderate level of motor, language, and cognitive disability.

Family 3 includes two affected siblings (subjects 3-3 and 3-4, Figure 1C) who are of Dutch descent and were born to asymptomatic parents. Both subjects presented with developmental delay, mild spastic ataxia, a wide-based gait, pyramidal signs, liver steatosis, and thin hair (Figures 3C and 3D). Polarized microscopy of hair shafts revealed trichorrhexis and moderate tiger-tail patterns in subject 3-3 (Figure 4D) and mild tiger-tail patterns in subject 3-4 (data not shown). Subject 3-3 was observed from infancy because of unexplained failure to thrive, cholestasis, and fat malabsorption and had complex partial and generalized seizures. Subject 3-4 presented at two months with congenital nystagmus and high myopia; at nine months she had repeated convulsions associated with fever and was diagnosed with hepatomegaly and steatosis. Brain CT of subject 3-3 revealed hemiatrophy and a wide right ventricle (data not shown). Subject 3-3 is currently 25 years old and has a moderate level of motor, language, and cognitive disability. Subject 3-4 is currently 20 years old and has a mild level of motor, language, and cognitive disability. Tiger-tail structural anomalies are typical of individuals affected by trichothiodystrophy (TTD);[34] indeed, this was the initial clinical diagnosis of subject 2-4. Because TTD is often caused by DNA-repair defects, thorough analysis of DNA-repair capacity was performed on skin fibroblasts from subjects 1-3, 2-4, and 3-3. This analysis did not reveal any defects (Figure S2).

To identify candidate variants for the unexplained phenotypes observed in our subjects, we performed exome sequencing (ES) on all affected individuals and their unaffected parents (Figure 1A–1C). In Family 1, ES was performed using the Illumina HiSeq2000 platform and the TrueSeq capture kit as previously described.[35–38] Sequence data were aligned to the human reference genome (hg19), and variants were filtered with VarSifter[39] on the basis of allele frequencies in the NIH-UDP cohort.[36,40,41] In families 2 and 3, trio ES was performed after DNA enrichment with Agilent Sureselect Exome V4 Capture and subsequently run on the HiSeq platform (101bp paired-end, Illumina) with an average depth coverage of 50×–100×; sequences were mapped with BWA. Variants were detected with the Genome Analysis Toolkit, and the VCF files were filtered with Cartagenia software (version 3.0.7). A summary of the ES analysis is provided in Table S2.

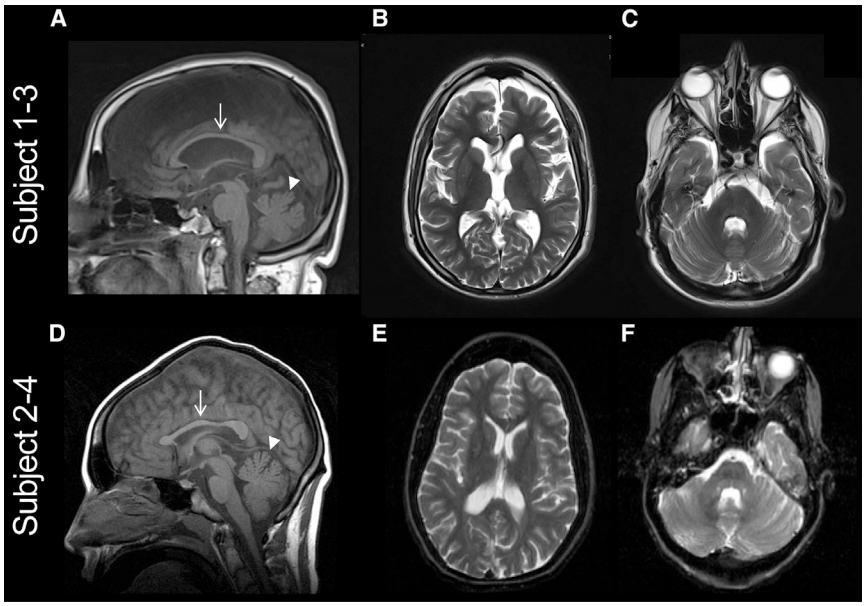

Figure 2. Subjects with *CARS* Variants Present with Central Nervous System Features
Sagittal T1-weighted (A) and axial T2-weighted (B and C) imaging of subject 1-3 shows moderate cerebral atrophy, a thin corpus callosum (A; arrow), mild atrophy of the superior cerebellar vermis (A; arrowhead), thin cerebellar folia, incomplete falx cerebri, incomplete tentorium, and variant anatomy of the circle of Willis. Sagittal T1-weighted imaging on subject 2-4 shows thin splenium of corpus callosum (D; arrow) and mild atrophy of the vermis (D; arrowhead). T2-weighted axial images of subject 2-4 show moderate global cerebral atrophy, deep sulci (E), thin cerebellar folia (F), and decreased white-matter volume, but globally normal myelination (D–F).

Analysis of ES data revealed that all four affected individuals are homozygous or compound heterozygous for *CARS* variants (Table 1 and Figure 1). Variant analysis by ES in family 1 revealed additional candidate disease-causing variants in *DEAF1* (MIM: 602635), *SOX30* (MIM: 606698), and *PTPN13* (MIM: 600267). In family 2, ES analysis revealed no additional candidate variants. In family 3, ES analysis revealed candidate variants in *ZNF185* (MIM: 300381). Importantly, the phenotypic similarity among subjects is consistent with the finding that all three families carry *CARS* variants, which were the only common candidates identified via ES; it should be noted that the research groups studying these families were connected via GeneMatcher[42] on the basis of the detection of *CARS* variants.

Sanger sequencing analysis of genomic DNA isolated from subjects' fibroblasts confirmed each variant (Figures 1 and 5A). Subject 1-3 is homozygous for c.2061dup, which predicts a frameshift variant, p.Ser688Glnfs*2 (Table 1). This variant is present in the gnomAD database[43]

Figure 3. Subjects with *CARS* Variants Present with Brittle Hair
Photographs show the brittle scalp hair in subject 1-3 (A), subject 2-4 (B), subject 3-3 (C), and subject 3-4 (D).

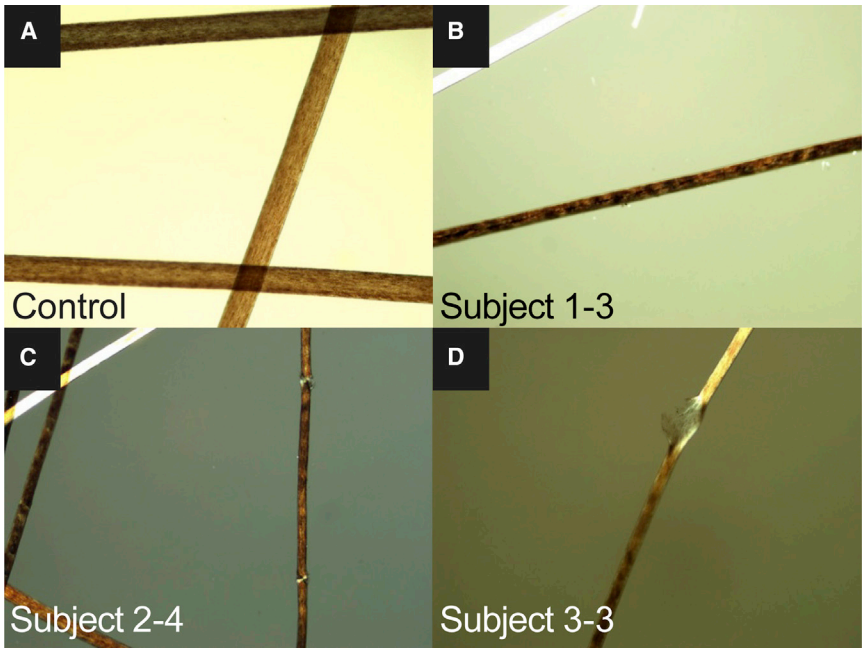

Figure 4. Subjects with *CARS* Variants Present with Hair-Shaft Abnormalities
Polarized light microscopy of hair shafts at the same magnification. Depicted are:
(A) An unrelated, age-matched healthy subject.
(B) Subject 1-3, showing moderate tiger-tail patterns.
(C) Subject 2-4, showing trichorrhexis and tiger-tail patterns.
(D) Subject 3-3, showing trichorrhexis and moderate tiger-tail patterns.
Note the difference in shaft diameter between healthy (A) and affected (B–D) subjects.

only in the heterozygous state (2/251,406). Subject 2-4 is compound heterozygous for two *CARS* variants. The maternally inherited variant (c.1022G>A; p.Arg341His) is present in gnomAD (8/178,368); however, no homozygous individuals were detected in this database (Table 1). The paternally inherited variant (c.1138C>T; p.Gln380*) is present in gnomAD with a very low frequency (1/184,276) (Table 1). Subjects 3-3 and 3-4 are both compound heterozygous for two *CARS* missense variants. The maternally inherited variant (c.1076C>T; p.Ser359Leu) is present in the gnomAD database (8/194,406); however, no homozygous individuals were detected (Table 1). The paternally inherited variant (c.1199T>A; p.Leu400Gln) is not present in the gnomAD database (Table 1).

CARS is the sole enzyme responsible for charging $tRNA^{Cys}$ molecules in the cytoplasm of mammalian cells; CARS2 is a nuclear-encoded enzyme responsible for charging $tRNA^{Cys}$ molecules in mitochondria.[1] There are two protein isoforms of CARS; they differ in their C-terminal sequences and result from alternative splicing of the penultimate exon.[44] CARS is a class I ARS enzyme containing a catalytic domain that activates and transfers cysteine to tRNA. CARS also contains an anticodon binding domain for tRNA recognition.[45–47] The p.Arg341His, p.Ser359Leu, p.Gln380*, and p.Leu400Gln variants all affect residues that map to the catalytic domain (Figure 5B). The p.Gln380* variant is predicted to result in a truncated protein missing 368 of the 748 CARS amino acid residues; such a truncation would result in the complete loss of the anticodon-binding domain. The p.Ser688Glnfs*2 variant maps to the C terminus in a region that is conserved among eukaryotes and that is important for the binding specificity between CARS and $tRNA^{Cys}$.[48] We assessed the evolutionary conservation of each affected CARS amino acid residue by aligning protein sequences of CARS orthologs from multiple species. The Arg341 residue is conserved among all analyzed species; the Leu400 residue is conserved in all analyzed species except bacteria; and the Ser359 residue is conserved among the human, mouse, and zebrafish CARS proteins (Figure 5C). The p.Ser688Glnfs*2 variant is predicted to truncate CARS by 60 amino acids. Of those 60 amino acids, 28% (17/60) are conserved among all analyzed species except bacteria, and 70% (42/60) are conserved among the human, mouse, and zebrafish CARS proteins (Figure 5C and data not shown).

Table 1. *CARS* Variants Identified in Subjects with Recessive Disease

Subject	Nucleotide Change[a]	Amino Acid Change[b]	Detection in gnomAD[c]	Minor-Allele Frequency
1-3	c.2061dup	p.Ser688Glnfs*2	2/251,406	0.000008
2-4	c.1022G>A	p.Arg341His	8/178,368	0.00004
2-4	c.1138C>T	p.Gln380*	1/184,276	0.000005
3-3	c.1076C>T	p.Ser359Leu	8/194,406	0.00004
3-3	c.1199T>A	p.Leu400Gln	Not present	0

[a]Human nucleotide positions correspond to GenBank: NM_001751.5.
[b]Human amino acid positions correspond to GenBank: NP_001742.1.
[c]See Web Resources.

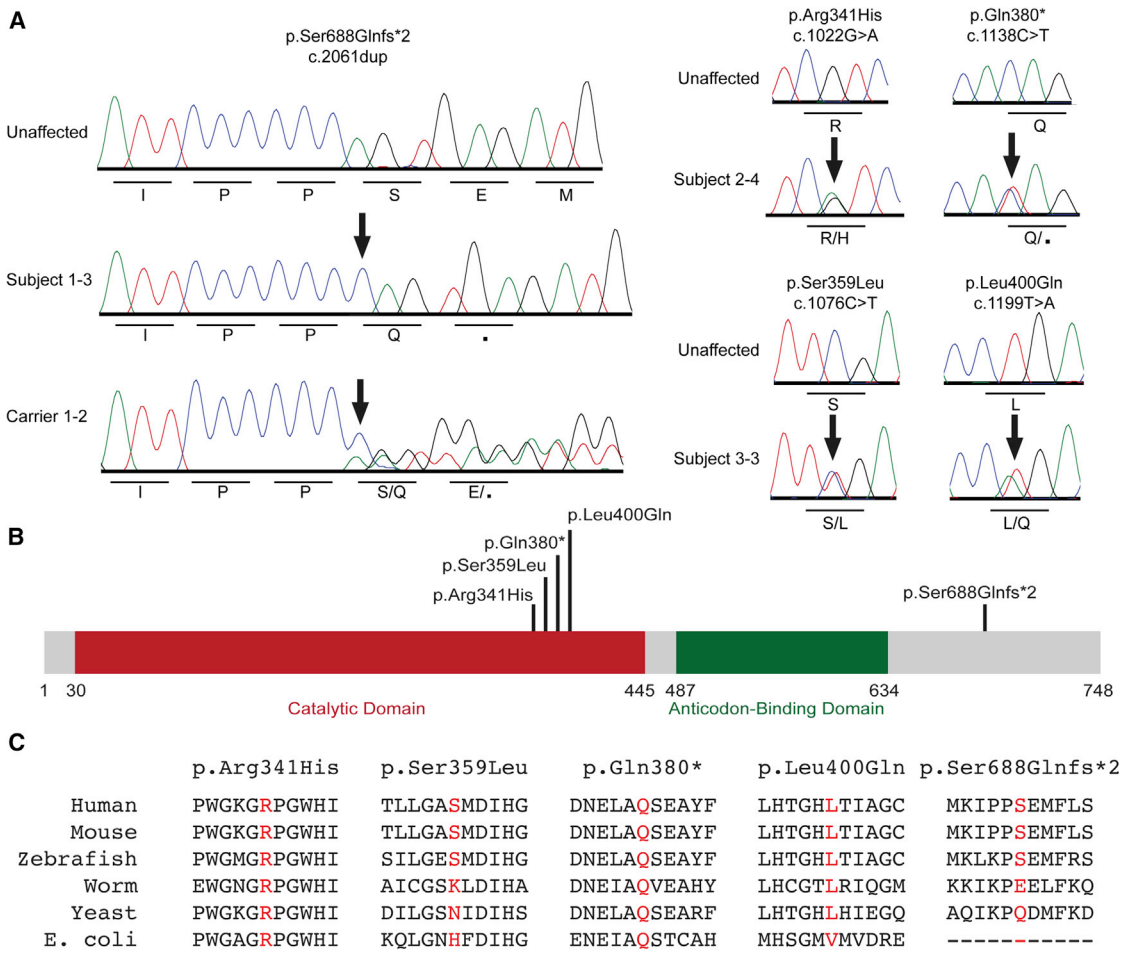

Figure 5. Characterization of *CARS* Variants Identified in the Cohort of Affected Subjects
(A) Representative sequence chromatograms are shown for the individuals indicated on the left. The protein and cDNA annotations of the identified variants are above, and the effect on amino acid sequence is indicated below. Arrows show the position of each variant.
(B) CARS functional domains are indicated in red (catalytic domain) and green (anticodon-binding domain) and the positions of the variants are shown across the top. Numbers along the bottom indicate amino acid positions for the CARS protein.
(C) The position of each variant is shown along with flanking CARS amino acid residues from multiple evolutionarily diverse species. The protein annotation of the variant is above, and the species names are on the left. The position of the affected residue is shown in red for each species.

The p.Gln380* and p.Ser688Glnfs*2 *CARS* variants encode premature stop codons and are therefore predicted to reduce the expression of full-length CARS. To test this prediction, we performed immunoblot analyses on protein isolated from fibroblasts from both affected individuals and unaffected controls; for these analyses, we used antibodies against CARS (sc-390230, Santa Cruz, purified mouse antibody, 1:250 dilution) and actin (A5060, Sigma, purified rabbit antibody, 1:5000 dilution). The molecular weights of the two wild-type CARS isoforms are predicted to be ~82 kDa and ~85 kDa;[44] these isoforms appear as a single band when lysates are electrophoresed on a 4%–20% tris-glycine gel (Figure 6A). In protein isolated from subject 1-3's fibroblasts, there was a single band at ~78 kDa, consistent with the predicted size of the truncated protein (Figure 6A). We therefore conclude that a truncated protein is expressed and stable, which is consistent with the viability of subject 1-3. In protein isolated from subject 2-4's fibroblasts, the amount of full-length CARS protein were significantly reduced in comparison to the amount in control cells (Figure 6A). This could be explained by the ablation of the expression of full-length CARS by the p.Gln380* variant; no truncated protein was detectable upon repeated analysis of an entire blot (Figure S3). In protein isolated from subject 3-3's fibroblasts, the amount of full-length CARS protein was similar to that of control cells (Figure 6A), which is consistent with the expression of two expressed and stable missense CARS protein variants in this subject. To determine whether the identified *CARS* variants affect subcellular protein localization, we performed immunofluorescence analysis by using a CARS antibody (H00000833-B01P, Novus Biologicals). These studies did not reveal any gross changes in CARS protein localization (Figure S4).

To assess the effect of *CARS* variants in the context of the affected individuals' genotypes, we performed steady-state

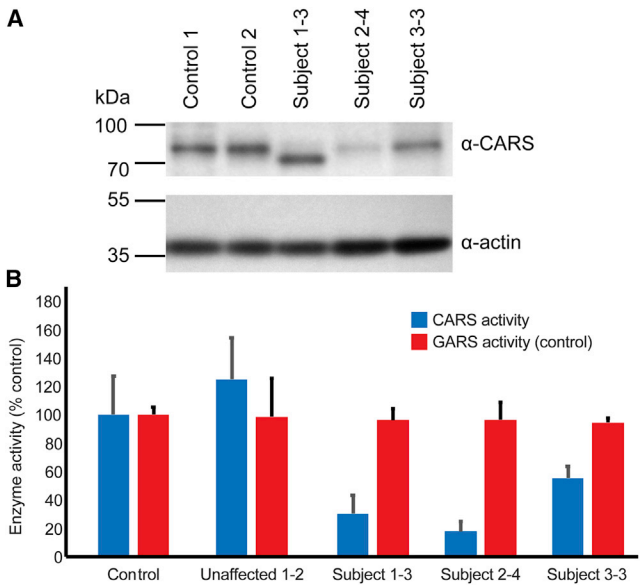

Figure 6. *CARS* Variants Affect Gene Function in Cell Lines from Affected Subjects

(A) Immunoblot analyses were performed on total protein lysates that were isolated from fibroblasts and through the use of an anti-CARS or anti-actin antibody (indicated on the right). Sample names are across the top, and sizes (kDa) are indicated at the left. Analysis revealed a truncated CARS protein in cells from subject 1-3 and reduced CARS protein expression in cells from subject 2-4 compared to controls.

(B) The cytosolic fraction of subjects' fibroblasts was used to determine CARS (blue) and GARS (red; internal control) activities. Samples are labeled across the bottom, and error bars indicate standard deviations of three technical replicates.

aminoacylation reactions on protein lysates from fibroblasts taken from those individuals. GARS activity was simultaneously measured as an internal control. In brief, assays were performed at 37°C in reaction buffer (50 mmol/L Tris buffer [pH 7.5], 12 mmol/L MgCl, 25 mol/L KCl, 1 mg/mL bovine serum albumin, 0.5 mmol/L spermine, 1 mmol/L ATP, 0.2 mmol/L yeast total tRNA, 1 mmol/L dithiotreitol, and 0.3 mM [13C4,15N] cysteine and [D2] glycine). The reaction was terminated with trichloroacetic acid (TCA). After reaction termination and washing, ammonia was added so that [13C4,15N] cysteine and [D2] glycine would be released from tRNA molecules. [13C2,15N] glycine was added as an internal standard. Labeled amino acids were quantified by liquid chromatography-tandem mass spectrometry (LC-MS/MS). Intra-assay variation was <15%, and no decreases were observed for GARS (internal control) activity in affected versus unaffected individuals (p value = 0.624). Statistical significance was determined with a one-tailed, unpaired t test. Compared to control cells and those isolated from the unaffected mother in family 1, each subject showed significantly reduced CARS activity (Figure 6B; p value < 0.001): ~70% reduction for subject 1-3, ~80% reduction for subject 2-4, and ~40% reduction for subject 3-3. Importantly, these data are consistent with a loss-of-function effect for each *CARS* variant.

To evaluate the functional consequences of each *CARS* allele in isolation, we developed a yeast complementation assay. In brief, a haploid yeast strain was generated with the endogenous yeast *CARS* ortholog (*YNL247W*) deleted, and viability was maintained with *YNL247W* on a *URA3*-bearing maintenance vector. Each *CARS* variant was modeled in human *CARS*, which was reported to rescue loss of *YNL247W*.[49] Wild-type or mutant *CARS* (or wild-type *YNL247W*) was transformed into yeast, and growth was evaluated on 5-FOA medium, which selects for the spontaneous loss of the maintenance vector.[50] The amount of CARS protein present in transformed yeast was assessed via immunoblot analysis (Figure S5). Wild-type *YNL247W* and wild-type human *CARS* rescued yeast viability, whereas an empty vector did not (Figure 7A). This is consistent with the finding that human *CARS* supports loss of the endogenous *YNL247W* and with *YNL247W* being an essential gene, respectively. The p.Gln380*, p.Leu400Gln, and p.Ser688Glnfs*2 variants did not support any yeast cell growth (Figure 7A), consistent with a loss-of-function effect. The p.Arg341His and p.Ser359Leu variants were associated with severely reduced but not ablated yeast cell growth (Figure 7A), consistent with hypomorphic alleles. To gain a more sensitive assessment of the hypomorphic p.Arg341His or p.Ser359Leu variants, we performed aminoacylation assays, which evaluate the kinetic properties of ARS variants and have been established as informative for studying disease-associated ARS alleles.[51] We tested recombinant human CARS proteins (wild-type, p.Arg341His, and p.Ser359Leu) for the ability to charge human cytoplasmic $tRNA^{Cys}$ with ^{35}S-labeled cysteine as previously described.[44,52] Analysis of the initial rate of aminoacylation as a function of the tRNA substrate concentration showed that both mutant CARS proteins cause a reduction in enzyme activity (Figure 7B and Table S3): p.Arg341His resulted in a 50% reduction in activity compared to that of wild-type CARS, and p.Ser359Leu resulted in a 84% reduction in activity compared to that of wild-type CARS. These data are consistent with the yeast complementation assay and the skin fibroblast results and indicate that each of these variants is a hypomorphic allele.

In summary, we present clinical, genetic, and functional data that implicate *CARS* variants in a multi-system, recessive disease that includes microcephaly, developmental delay, and brittle hair and nails. The genetic and clinical evidence we present supports the pathogenicity of the identified *CARS* variants in several ways. First, three independent pedigrees displayed an overlapping phenotype with unique features, including brittle hair and nails; these data are consistent with a common underlying genetic etiology among the three families. Second, *CARS* variants segregate with the presumed recessive phenotype in all three families, and each affected subject is homozygous or compound heterozygous for variants that result in truncated proteins or that affect highly conserved amino acids. Third, our functional studies also strongly support the

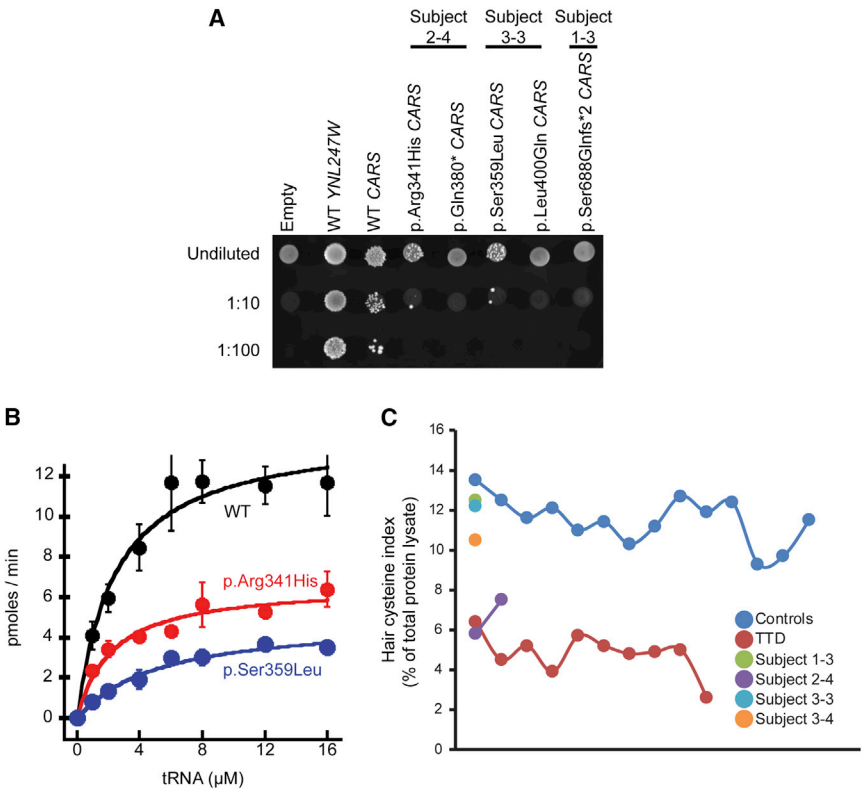

Figure 7. All Five Disease-Associated *CARS* Variants Cause Loss-of-Function Effects

(A) Haploid yeast cells lacking endogenous *YNL247W* (the yeast ortholog of *CARS*) were transformed with vectors containing wild-type or mutant *CARS* or with a vector with no *CARS* insert ("empty"); the vector used in each experiment is indicated across the top. Resulting cultures, either undiluted or diluted (1:10 or 1:100), were plated on solid growth medium containing 5-FOA and grown at 30°C for 5 days. The corresponding affected individual who carries each variant is listed above.

(B) Initial aminoacylation rates (pmol/min) of wild-type (black circles and line), p.Arg341His (red circles and lines), and p.Ser359Leu (blue circles and line) CARS were plotted against tRNA concentrations and fit to the Michaelis-Menten equation. Error bars indicate standard deviations of three technical replicates.

(C) Hair cysteine index (percent of total protein lysate) in controls and TTD-affected individuals compared to individuals with bi-allelic *CARS* variants. Note that only subject 2-4 (two independent samples) falls within the range of TTD subjects. Only one sample each was assessed for subject 1-3, subject 3-3, and subject 3-4.

pathogenicity of each *CARS* variant. Specifically, each variant causes a loss-of-function effect in protein abundance, tRNA charging, or yeast complementation assays. Indeed, these assays are commonly used for demonstrating a loss-of-function effect for disease-associated ARS mutations. Aminoacylation assays have tested the effects of variants in 15 ARS genes implicated in recessive disease, and yeast complementation assays have tested the effects of variants in eight ARS genes implicated in recessive disease.[51] Using cell lysates from affected individuals to test aminoacylation activity is a technique that determines the effects of ARS mutations in the context of the affected individual's genome; these studies will be critical for future efforts to better classify the effect of disease-associated ARS genotypes on tRNA charging.

Our functional studies on the disease-associated *CARS* variants also provide insight into the pathogenic mechanism of the clinical phenotype observed in our subjects. That is, the loss-of-function effects suggest that impaired tRNA charging leads to reduced, interrupted, or otherwise altered protein translation in the affected organ systems. This notion is consistent with previous reports of loss-of-function effects of variants in other ARS genes identified in individuals with recessive phenotypes.[2] An alternative—albeit less likely—possibility is that CARS has some non-canonical function that is unrelated to tRNA charging and that is affected by the variants described here, and that this function is particularly important for the affected tissues. Although CARS has been reported to function in cysteine polysulfidation[53] and ferroptosis,[54] further work is needed to identify secondary CARS functions that might be relevant to the phenotypes in our subjects. Importantly, phenotypic overlap between our subjects and others with ARS-mediated recessive disease further supports the pathogenicity of the identified *CARS* variants and indicates a common mechanism for ARS-related recessive disease. Indeed, the combination of clinical features in our subjects is compatible with what has previously been reported in other ARS-related autosomal-recessive phenotypes. For example, developmental delay is common to all four individuals with *CARS* variants and is also seen in individuals with variants in *DARS* (MIM: 603084), *DARS2* (MIM: 610956), *FARS2* (MIM: 611592), *KARS* (MIM: 601421), *NARS2* (MIM: 612803), *PARS2* (MIM: 612036), *QARS* (MIM: 603727), *RARS2* (MIM: 611524), *VARS* (MIM: 192150), and *YARS* (MIM: 603623).[2] Similarly, microcephaly is common to subjects 1-3 and 2-4 and is also seen in individuals with variants in *AARS* (MIM: 601065), *GARS* (MIM: 600287), *IARS* (MIM: 600709), *KARS*, *NARS2*, *PARS2*, *QARS*, *RARS2*, *SARS* (MIM: 607529), *VARS*, *VARS2* (MIM: 612802), and *WARS2* (MIM: 604733).[2,55] Finally, liver dysfunction is common to subjects 1-3, 3-3, and 3-4 and is also seen in individuals with variants in *EARS2* (MIM: 612799), *FARSB* (MIM: 609690), *FARS2*, *IARS*, *LARS* (MIM: 151350), *LARS2* (MIM: 604544), *MARS* (MIM: 156560), and *YARS*.[2,3,7,9,56,57] In addition to the above phenotypes, subject 1-3 has an axonal peripheral neuropathy, which has previously been associated with variants in five other ARS loci.[2] Severe depletion of tRNA charging might be responsible for the peripheral neuropathy in this

individual; reduced enzyme function is a common feature of neuropathy-associated ARS variants.[2,51]

Interestingly, all four affected individuals described here have some degree of fine, brittle hair with microscopic shaft abnormalities; this characteristic has not been previously associated with disease-causing ARS variants. Hair and nails could be particularly susceptible to impairments in CARS function because of the high cysteine content of keratins expressed in these tissues. To begin to address this possibility, we performed quantitative analysis of hair amino acid composition after hydrolysis and followed this with liquid chromatography. Consistent with our hypothesis, this assay showed a lower cysteine to total amino acid index in hair from subject 2-4, which is within the range for individuals with TTD (Figure 7C). No other individual in our study showed such an effect on the hair cysteine index, but it is interesting to note that subject 2-4 had both the most abnormal hair structure and the most dramatic reduction in CARS activity (Figure 6B). At the moment, it is not clear why CARS deficiency renders individuals susceptible to other characteristic phenotypes such as liver steatosis and impairment of the central nervous system. Confirming our observations and determining whether the translation of cysteine-rich proteins is affected by impaired CARS activity will require further studies in appropriate animal models.

In conclusion, we present clinical, genetic, and functional data that implicate *CARS* variants in a multi-system, recessive disease that includes microcephaly, developmental delay, and brittle hair and nails. These findings expand the locus and clinical heterogeneity of ARS-related disease and further support the hypothesis that impaired tRNA charging followed by protein translation defects is the primary pathogenic mechanism of ARS-related recessive disease.

Supplemental Data

Supplemental Data can be found with this article online at https://doi.org/10.1016/j.ajhg.2019.01.006.

Acknowledgments

M.K. is supported by the NIH Medical Scientist Training Program Training Grant (GM007863) and the NIH Cellular and Molecular Biology Training Grant (GM007315). A.F.T., A.R., and W. V. are supported by a European Research Council Advanced Grant (340988-ERC-ID). M.I.M is supported by the European Leukodystrophies Association. R.M. is supported by an NIH F31 NRSA (NS108510) and the Michigan Pre-Doctoral Training in Genetics Program (GM007544). This study is partly supported by the NHGRI Intramural Research Program of the National Institutes of Health and the Common Fund from the NIH Office of the Director. Y.M.H. is supported by grants from the National Institute of General Medical Sciences (GM108972, GM114343, GM126210). A.A. is supported by a grant from the National Institute of General Medical Sciences (GM118647). G.M.S.M. is supported by private donations, by the Erasmus MC Mrace grant 104673 and ZonMW Top grant 1827002. The authors would like to thank Yan Huang and Valerie Maduro (NHGRI, NIH) for their assistance in establishing and maintaining the cells from subject 1-3 and his parent, and William Bone and Catherine Chao (NHGRI) for their assistance in bioinformatic analysis. We also thank Dr. Maarten H. Lequin (Urecht Academic Medical Center) for discussion of the MRI findings.

Declaration of Interests

The authors declare no competing interests.

Received: December 6, 2018
Accepted: January 15, 2019
Published: February 28, 2019

Web Resources

BWA, http://bio-wa.sourceforge.net/
Clustal Omega, https://www.ebi.ac.uk/Tools/msa/clustalo/
GenBank, http://www.ncbi.nlm.nih.gov/genbank/
GeneMatcher, https://www.genematcher.org
Genome Analysis Toolkit, http://www.broadinstitute.org/gatk/
gnomAD, http://gnomad.broadinstitute.org
OMIM, https://www.omim.org

References

1. Antonellis, A., and Green, E.D. (2008). The role of aminoacyl-tRNA synthetases in genetic diseases. Annu. Rev. Genomics Hum. Genet. *9*, 87–107.
2. Meyer-Schuman, R., and Antonellis, A. (2017). Emerging mechanisms of aminoacyl-tRNA synthetase mutations in recessive and dominant human disease. Hum. Mol. Genet. *26* (R2), R114–R127.
3. Antonellis, A., Oprescu, S.N., Griffin, L.B., Heider, A., Amalfitano, A., and Innis, J.W. (2018). Compound heterozygosity for loss-of-function FARSB variants in a patient with classic features of recessive aminoacyl-tRNA synthetase-related disease. Hum. Mutat. *39*, 834–840.
4. Mendes, M.I., Gutierrez Salazar, M., Guerrero, K., Thiffault, I., Salomons, G.S., Gauquelin, L., Tran, L.T., Forget, D., Gauthier, M.-S., Waisfisz, Q., et al. (2018). Bi-allelic mutations in EPRS, encoding the glutamyl-prolyl-aminoacyl-trna synthetase, cause a hypomyelinating leukodystrophy. Am. J. Hum. Genet. *102*, 676–684.
5. Nakayama, T., Wu, J., Galvin-Parton, P., Weiss, J., Andriola, M.R., Hill, R.S., Vaughan, D.J., El-Quessny, M., Barry, B.J., Partlow, J.N., et al. (2017). Deficient activity of alanyl-tRNA synthetase underlies an autosomal recessive syndrome of progressive microcephaly, hypomyelination, and epileptic encephalopathy. Hum. Mutat. *38*, 1348–1354.
6. Coughlin, C.R., 2nd, Scharer, G.H., Friederich, M.W., Yu, H.-C., Geiger, E.A., Creadon-Swindell, G., Collins, A.E., Vanlander, A.V., Coster, R.V., Powell, C.A., et al. (2015). Mutations in the mitochondrial cysteinyl-tRNA synthase gene, CARS2, lead to a severe epileptic encephalopathy and complex movement disorder. J. Med. Genet. *52*, 532–540.
7. Oliveira, R., Sommerville, E.W., Thompson, K., Nunes, J., Pyle, A., Grazina, M., Chinnery, P.F., Diogo, L., Garcia, P., and Taylor, R.W. (2017). Lethal neonatal LTBL associated with biallelic

EARS2 variants: Case report and review of the reported neuroradiological features. JIMD Rep. *33*, 61–68.
8. Schwartzentruber, J., Buhas, D., Majewski, J., Sasarman, F., Papillon-Cavanagh, S., Thiffault, I., Sheldon, K.M., Massicotte, C., Patry, L., Simon, M., et al.; FORGE Canada Consortium (2014). Mutation in the nuclear-encoded mitochondrial isoleucyl-tRNA synthetase IARS2 in patients with cataracts, growth hormone deficiency with short stature, partial sensorineural deafness, and peripheral neuropathy or with Leigh syndrome. Hum. Mutat. *35*, 1285–1289.
9. Riley, L.G., Rudinger-Thirion, J., Schmitz-Abe, K., Thorburn, D.R., Davis, R.L., Teo, J., Arbuckle, S., Cooper, S.T., Campagna, D.R., Frugier, M., et al. (2016). LARS2 variants associated with hydrops, lactic acidosis, sideroblastic anemia, and multisystem failure. JIMD Rep. *28*, 49–57.
10. Vanlander, A.V., Menten, B., Smet, J., De Meirleir, L., Sante, T., De Paepe, B., Seneca, S., Pearce, S.F., Powell, C.A., Vergult, S., et al. (2015). Two siblings with homozygous pathogenic splice-site variant in mitochondrial asparaginyl-tRNA synthetase (NARS2). Hum. Mutat. *36*, 222–231.
11. Simon, M., Richard, E.M., Wang, X., Shahzad, M., Huang, V.H., Qaiser, T.A., Potluri, P., Mahl, S.E., Davila, A., Nazli, S., et al. (2015). Mutations of human NARS2, encoding the mitochondrial asparaginyl-tRNA synthetase, cause nonsyndromic deafness and Leigh syndrome. PLoS Genet. *11*, e1005097.
12. Cassandrini, D., Cilio, M.R., Bianchi, M., Doimo, M., Balestri, M., Tessa, A., Rizza, T., Sartori, G., Meschini, M.C., Nesti, C., et al. (2013). Pontocerebellar hypoplasia type 6 caused by mutations in RARS2: Definition of the clinical spectrum and molecular findings in five patients. J. Inherit. Metab. Dis. *36*, 43–53.
13. Diodato, D., Melchionda, L., Haack, T.B., Dallabona, C., Baruffini, E., Donnini, C., Granata, T., Ragona, F., Balestri, P., Margollicci, M., et al. (2014). VARS2 and TARS2 mutations in patients with mitochondrial encephalomyopathies. Hum. Mutat. *35*, 983–989.
14. Baertling, F., Alhaddad, B., Seibt, A., Budaeus, S., Meitinger, T., Strom, T.M., Mayatepek, E., Schaper, J., Prokisch, H., Haack, T.B., and Distelmaier, F. (2017). Neonatal encephalocardiomyopathy caused by mutations in VARS2. Metab. Brain Dis. *32*, 267–270.
15. Sasarman, F., Nishimura, T., Thiffault, I., and Shoubridge, E.A. (2012). A novel mutation in YARS2 causes myopathy with lactic acidosis and sideroblastic anemia. Hum. Mutat. *33*, 1201–1206.
16. Danhauser, K., Haack, T.B., Alhaddad, B., Melcher, M., Seibt, A., Strom, T.M., Meitinger, T., Klee, D., Mayatepek, E., Prokisch, H., and Distelmaier, F. (2016). EARS2 mutations cause fatal neonatal lactic acidosis, recurrent hypoglycemia and agenesis of corpus callosum. Metab. Brain Dis. *31*, 717–721.
17. Jiang, P., Jin, X., Peng, Y., Wang, M., Liu, H., Liu, X., Zhang, Z., Ji, Y., Zhang, J., Liang, M., et al. (2016). The exome sequencing identified the mutation in YARS2 encoding the mitochondrial tyrosyl-tRNA synthetase as a nuclear modifier for the phenotypic manifestation of Leber's hereditary optic neuropathy-associated mitochondrial DNA mutation. Hum. Mol. Genet. *25*, 584–596.
18. Elo, J.M., Yadavalli, S.S., Euro, L., Isohanni, P., Götz, A., Carroll, C.J., Valanne, L., Alkuraya, F.S., Uusimaa, J., Paetau, A., et al. (2012). Mitochondrial phenylalanyl-tRNA synthetase mutations underlie fatal infantile Alpers encephalopathy. Hum. Mol. Genet. *21*, 4521–4529.
19. Walker, M.A., Mohler, K.P., Hopkins, K.W., Oakley, D.H., Sweetser, D.A., Ibba, M., Frosch, M.P., and Thibert, R.L. (2016). Novel compound heterozygous mutations expand the recognized phenotypes of FARS2-linked disease. J. Child Neurol. *31*, 1127–1137.
20. Puffenberger, E.G., Jinks, R.N., Sougnez, C., Cibulskis, K., Willert, R.A., Achilly, N.P., Cassidy, R.P., Fiorentini, C.J., Heiken, K.F., Lawrence, J.J., et al. (2012). Genetic mapping and exome sequencing identify variants associated with five novel diseases. PLoS ONE *7*, e28936.
21. Pierce, S.B., Chisholm, K.M., Lynch, E.D., Lee, M.K., Walsh, T., Opitz, J.M., Li, W., Klevit, R.E., and King, M.-C. (2011). Mutations in mitochondrial histidyl tRNA synthetase HARS2 cause ovarian dysgenesis and sensorineural hearing loss of Perrault syndrome. Proc. Natl. Acad. Sci. USA *108*, 6543–6548.
22. McLaughlin, H.M., Sakaguchi, R., Liu, C., Igarashi, T., Pehlivan, D., Chu, K., Iyer, R., Cruz, P., Cherukuri, P.F., Hansen, N.F., et al.; NISC Comparative Sequencing Program (2010). Compound heterozygosity for loss-of-function lysyl-tRNA synthetase mutations in a patient with peripheral neuropathy. Am. J. Hum. Genet. *87*, 560–566.
23. van Meel, E., Wegner, D.J., Cliften, P., Willing, M.C., White, F.V., Kornfeld, S., and Cole, F.S. (2013). Rare recessive loss-of-function methionyl-tRNA synthetase mutations presenting as a multi-organ phenotype. BMC Med. Genet. *14*, 106.
24. Zhang, X., Ling, J., Barcia, G., Jing, L., Wu, J., Barry, B.J., Mochida, G.H., Hill, R.S., Weimer, J.M., Stein, Q., et al. (2014). Mutations in QARS, encoding glutaminyl-tRNA synthetase, cause progressive microcephaly, cerebral-cerebellar atrophy, and intractable seizures. Am. J. Hum. Genet. *94*, 547–558.
25. Riley, L.G., Cooper, S., Hickey, P., Rudinger-Thirion, J., McKenzie, M., Compton, A., Lim, S.C., Thorburn, D., Ryan, M.T., Giegé, R., et al. (2010). Mutation of the mitochondrial tyrosyl-tRNA synthetase gene, YARS2, causes myopathy, lactic acidosis, and sideroblastic anemia–MLASA syndrome. Am. J. Hum. Genet. *87*, 52–59.
26. Simons, C., Griffin, L.B., Helman, G., Golas, G., Pizzino, A., Bloom, M., Murphy, J.L.P., Crawford, J., Evans, S.H., Topper, S., et al. (2015). Loss-of-function alanyl-tRNA synthetase mutations cause an autosomal-recessive early-onset epileptic encephalopathy with persistent myelination defect. Am. J. Hum. Genet. *96*, 675–681.
27. Dallabona, C., Diodato, D., Kevelam, S.H., Haack, T.B., Wong, L.-J., Salomons, G.S., Baruffini, E., Melchionda, L., Mariotti, C., Strom, T.M., et al. (2014). Novel (ovario) leukodystrophy related to AARS2 mutations. Neurology *82*, 2063–2071.
28. Orenstein, N., Weiss, K., Oprescu, S.N., Shapira, R., Kidron, D., Vanagaite-Basel, L., Antonellis, A., and Muenke, M. (2017). Biallelic IARS mutations in a child with intra-uterine growth retardation, neonatal cholestasis, and mild developmental delay. Clin. Genet. *91*, 913–917.
29. Kopajtich, R., Murayama, K., Janecke, A.R., Haack, T.B., Breuer, M., Knisely, A.S., Harting, I., Ohashi, T., Okazaki, Y., Watanabe, D., et al. (2016). Biallelic IARS mutations cause growth retardation with prenatal onset, intellectual disability, muscular hypotonia, and infantile hepatopathy. Am. J. Hum. Genet. *99*, 414–422.
30. Pierce, S.B., Gersak, K., Michaelson-Cohen, R., Walsh, T., Lee, M.K., Malach, D., Klevit, R.E., King, M.-C., and Levy-Lahad, E. (2013). Mutations in LARS2, encoding mitochondrial leucyl-tRNA synthetase, lead to premature ovarian failure and hearing loss in Perrault syndrome. Am. J. Hum. Genet. *92*, 614–620.

31. Hadchouel, A., Wieland, T., Griese, M., Baruffini, E., Lorenz-Depiereux, B., Enaud, L., Graf, E., Dubus, J.C., Halioui-Louhaichi, S., Coulomb, A., et al. (2015). Biallelic mutations of methionyl-tRNA synthetase cause a specific type of pulmonary alveolar proteinosis prevalent on Réunion Island. Am. J. Hum. Genet. *96*, 826–831.
32. Sommerville, E.W., Ng, Y.S., Alston, C.L., Dallabona, C., Gilberti, M., He, L., Knowles, C., Chin, S.L., Schaefer, A.M., Falkous, G., et al. (2017). Clinical features, molecular heterogeneity, and prognostic implications in YARS2-related mitochondrial myopathy. JAMA Neurol. *74*, 686–694.
33. Ardissone, A., Lamantea, E., Quartararo, J., Dallabona, C., Carrara, F., Moroni, I., Donnini, C., Garavaglia, B., Zeviani, M., and Uziel, G. (2015). A novel homozygous YARS2 mutation in two Italian siblings and a review of literature. JIMD Rep. *20*, 95–101.
34. Cheng, S., Stone, J., and de Berker, D. (2009). Trichothiodystrophy and fragile hair: The distinction between diagnostic signs and diagnostic labels in childhood hair disease. Br. J. Dermatol. *161*, 1379–1383.
35. Bentley, D.R., Balasubramanian, S., Swerdlow, H.P., Smith, G.P., Milton, J., Brown, C.G., Hall, K.P., Evers, D.J., Barnes, C.L., Bignell, H.R., et al. (2008). Accurate whole human genome sequencing using reversible terminator chemistry. Nature *456*, 53–59.
36. Gahl, W.A., Markello, T.C., Toro, C., Fajardo, K.F., Sincan, M., Gill, F., Carlson-Donohoe, H., Gropman, A., Pierson, T.M., Golas, G., et al. (2012). The National Institutes of Health Undiagnosed Diseases Program: insights into rare diseases. Genet. Med. *14*, 51–59.
37. Gnirke, A., Melnikov, A., Maguire, J., Rogov, P., LeProust, E.M., Brockman, W., Fennell, T., Giannoukos, G., Fisher, S., Russ, C., et al. (2009). Solution hybrid selection with ultra-long oligonucleotides for massively parallel targeted sequencing. Nat. Biotechnol. *27*, 182–189.
38. Teer, J.K., Bonnycastle, L.L., Chines, P.S., Hansen, N.F., Aoyama, N., Swift, A.J., Abaan, H.O., Albert, T.J., Margulies, E.H., Green, E.D., et al.; NISC Comparative Sequencing Program (2010). Systematic comparison of three genomic enrichment methods for massively parallel DNA sequencing. Genome Res. *20*, 1420–1431.
39. Teer, J.K., Green, E.D., Mullikin, J.C., and Biesecker, L.G. (2012). VarSifter: visualizing and analyzing exome-scale sequence variation data on a desktop computer. Bioinformatics *28*, 599–600, web39.
40. Gahl, W.A., and Tifft, C.J. (2011). The NIH Undiagnosed Diseases Program: lessons learned. JAMA *305*, 1904–1905.
41. Markello, T.C., Han, T., Carlson-Donohoe, H., Ahaghotu, C., Harper, U., Jones, M., Chandrasekharappa, S., Anikster, Y., Adams, D.R., Gahl, W.A., Boerkoel, C.F.; and NISC Comparative Sequencing Program (2012). Recombination mapping using Boolean logic and high-density SNP genotyping for exome sequence filtering. Mol. Genet. Metab. *105*, 382–389.
42. Sobreira, N., Schiettecatte, F., Boehm, C., Valle, D., and Hamosh, A. (2015). New tools for Mendelian disease gene identification: PhenoDB variant analysis module; and GeneMatcher, a web-based tool for linking investigators with an interest in the same gene. Hum. Mutat. *36*, 425–431.
43. Lek, M., Karczewski, K.J., Minikel, E.V., Samocha, K.E., Banks, E., Fennell, T., O'Donnell-Luria, A.H., Ware, J.S., Hill, A.J., Cummings, B.B., et al.; Exome Aggregation Consortium (2016). Analysis of protein-coding genetic variation in 60,706 humans. Nature *536*, 285–291.
44. Davidson, E., Caffarella, J., Vitseva, O., Hou, Y.M., and King, M.P. (2001). Isolation of two cDNAs encoding functional human cytoplasmic cysteinyl-tRNA synthetase. Biol. Chem. *382*, 399–406.
45. Finn, R.D., Attwood, T.K., Babbitt, P.C., Bateman, A., Bork, P., Bridge, A.J., Chang, H.-Y., Dosztányi, Z., El-Gebali, S., Fraser, M., et al. (2017). InterPro in 2017-beyond protein family and domain annotations. Nucleic Acids Res. *45* (D1), D190–D199.
46. Liu, C., Sanders, J.M., Pascal, J.M., and Hou, Y.-M. (2012). Adaptation to tRNA acceptor stem structure by flexible adjustment in the catalytic domain of class I tRNA synthetases. RNA *18*, 213–221.
47. Marchler-Bauer, A., Bo, Y., Han, L., He, J., Lanczycki, C.J., Lu, S., Chitsaz, F., Derbyshire, M.K., Geer, R.C., Gonzales, N.R., et al. (2017). CDD/SPARCLE: Functional classification of proteins via subfamily domain architectures. Nucleic Acids Res. *45* (D1), D200–D203.
48. Liu, C., Gamper, H., Shtivelband, S., Hauenstein, S., Perona, J.J., and Hou, Y.-M. (2007). Kinetic quality control of anticodon recognition by a eukaryotic aminoacyl-tRNA synthetase. J. Mol. Biol. *367*, 1063–1078.
49. Kachroo, A.H., Laurent, J.M., Yellman, C.M., Meyer, A.G., Wilke, C.O., and Marcotte, E.M. (2015). Evolution. Systematic humanization of yeast genes reveals conserved functions and genetic modularity. Science *348*, 921–925.
50. Boeke, J.D., LaCroute, F., and Fink, G.R. (1984). A positive selection for mutants lacking orotidine-5′-phosphate decarboxylase activity in yeast: 5-fluoro-orotic acid resistance. Mol. Gen. Genet. *197*, 345–346.
51. Oprescu, S.N., Griffin, L.B., Beg, A.A., and Antonellis, A. (2017). Predicting the pathogenicity of aminoacyl-tRNA synthetase mutations. Methods *113*, 139–151.
52. Hou, Y.M., Westhof, E., and Giegé, R. (1993). An unusual RNA tertiary interaction has a role for the specific aminoacylation of a transfer RNA. Proc. Natl. Acad. Sci. USA *90*, 6776–6780.
53. Akaike, T., Ida, T., Wei, F.-Y., Nishida, M., Kumagai, Y., Alam, M.M., Ihara, H., Sawa, T., Matsunaga, T., Kasamatsu, S., et al. (2017). Cysteinyl-tRNA synthetase governs cysteine polysulfidation and mitochondrial bioenergetics. Nat. Commun. *8*, 1177.
54. Hayano, M., Yang, W.S., Corn, C.K., Pagano, N.C., and Stockwell, B.R. (2016). Loss of cysteinyl-tRNA synthetase (CARS) induces the transsulfuration pathway and inhibits ferroptosis induced by cystine deprivation. Cell Death Differ. *23*, 270–278.
55. Oprescu, S.N., Chepa-Lotrea, X., Takase, R., Golas, G., Markello, T.C., Adams, D.R., Toro, C., Gropman, A.L., Hou, Y.-M., Malicdan, M.C.V., et al. (2017). Compound heterozygosity for loss-of-function GARS variants results in a multisystem developmental syndrome that includes severe growth retardation. Hum. Mutat. *38*, 1412–1420.
56. Peroutka, C., Salas, J., Britton, J., Bishop, J., Kratz, L., Gilmore, M.M., Fahrner, J.A., Golden, W.C., and Wang, T. (2019). Severe neonatal manifestations of Infantile Liver Failure Syndrome Type 1 caused by cytosolic leucine-tRNA synthetase deficiency. JIMD Rep. *45*, 71–76.
57. Xu, Z., Lo, W.-S., Beck, D.B., Schuch, L.A., Oláhová, M., Kopajtich, R., Chong, Y.E., Alston, C.L., Seidl, E., Zhai, L., et al. (2018). Bi-allelic mutations in phe-tRNA synthetase associated with a multi-system pulmonary disease support non-translational function. Am. J. Hum. Genet. *103*, 100–114.